J Mater Sci (2008) 43:2006–2011
DOI 10.1007/s10853-008-2448-x

# Phase orientation, interface structure, and properties of aged Cu-6 wt.% Ag

**J. B. Liu · L. Meng**

Received: 17 September 2007 / Accepted: 4 January 2008 / Published online: 31 January 2008


**Abstract** The crystallographic orientation and interface structure of Ag precipitates were investigated for aged Cu-6 wt.% Ag. The hardness and resistivity were determined for the aged alloy for different times. Ag secondary particles form in the Cu matrix from a discontinuous precipitation and the precipitated cells extend with the increase in aging time. There are the cube-on-cube relationship and semi-coherent interface between the Ag precipitate and the Cu matrix. Some dislocations are regularly arranged at the interface. The improvements of the hardness and conductivity can mainly be attributed to the increase in interface strengthening and the decrease in solute scattering in the Cu matrix during aging treatment. The high lattice-matching level and regular dislocation arrangement at the interface produce high strain resistance and low electron scattering.

## Introduction

Cu–Ag alloys are the important candidates of conductor materials to manufacture the excitation windings of pulsed high-field magnets due to their excellent combination of strength and conductivity to endure Lorentz forces and minimize Joule heating [1–6]. Strong drawing deformation is an effective approach to produce the double-phase filamentary structure in the alloys. The strength determined from the filamentary structure is far higher than that predicted from the summation of phase components, while the electrical conductivity of the filamentary structure can still be retained at a relatively high level.

The microstructure of Cu–Ag alloys is usually composed of Cu matrix, eutectic colonies, and Ag precipitates. The Cu and Ag phases in different structure components should have different interface structure and phase orientation since both phases have different formation conditions in different structure components. For example, it was pointed out that there always was a cube-on-cube orientation relationship between both phases in all pro-eutectic regions but only in partial eutectic areas [7]. Many studies were also focused on the effect of structure component volume or interface density on the properties of Cu–Ag alloys [2, 8–10]. Sakai et al. [11] indicated that the precipitation reaction to form Ag secondary particles in intermediate heat treatments improved the strength and electrical conductivity of Cu-24 wt.% Ag. Han et al. [7] demonstrated that the strength of drawn Cu–Ag alloys was strongly dependent on the spacing between Ag fibers evolved from the Ag precipitates in pro-eutectic Cu dendrites. Hong and Hill [1] also suggested that the strength of the precipitation region could be calculated according to the average spacing of Ag precipitates. Our recent study [12] revealed that Ag precipitates could produce a similar strengthening effect in both Cu-6 wt.% Ag and Cu-12 wt.% Ag at low drawing strain levels although the Ag concentration in both alloys was evidently different.

As mentioned above, it is obvious that the interface between the Ag precipitate and the Cu matrix plays a main role in the strengthening and conducting behaviors for the composite structure of Cu and Ag fibers. Moreover, the interface characteristic of the filamentary structure is basically dependent on the primary status of interface formation. However, the crystallographic orientation and interface structure of original precipitates in Cu–Ag alloys

J. B. Liu · L. Meng (✉)
Department of Materials Science and Engineering,
Zhejiang University, Hangzhou 310027, China
e-mail: mengliang@zju.edu.cn

before the formation of filamentary structure is still understood insufficiently. High-resolution transmission electron microscopy (HRTEM) can effectively observe the interface characteristic and has been used to investigate the strengthening and conducting mechanisms related to the phase feature, interface structure, dislocation distribution, lattice defect, and crystallographic orientation in double-phase alloys, such as Cu–Nb and Cu–Ag [13–19]. In this paper, Cu-6 wt.% Ag was solution treated and aged to produce Ag precipitates. HRTEM was used to reveal the phase orientation and interface structure of Ag precipitates in the Cu matrix. The hardness and resistivity were determined for the alloy aged for different times in order to discuss the relationship of interface characteristics with the mechanical and electrical properties.

## Experiments

Cu-6 wt.% Ag was melted in a vacuum induction furnace and cast into cylindrical ingots in a copper mold. Metallic silver and electrolytic copper with the purity higher than 99.98% were used as starting materials. The ingots were solution treated at 720 °C for 4 h followed by water quenching and aged at 450 °C for different times to form Ag precipitates in super-saturated Cu dendrites.

The morphology of Ag precipitates was observed using a SIRRON200 field emission scanning electron microscope (FESEM). The phase orientation and interface structure between the Ag precipitate and the Cu matrix were examined using a JEM-2010 HRTEM operated at 200 kV. The TEM specimens were prepared by mechanically thinning and then ion milling at 5 kV with an incidence angle of 12°. The hardness was determined using a Vickers hardness tester with a load 100 g and holding time 15 s. The hardness value for each sample was taken from the arithmetical mean of the measured data more than ten indentations. The electrical resistivity was measured by a standard four-probe technique at ambient temperature.

## Results

The microstructure of the solution treated Cu-6 wt.% Ag contains the Cu matrix and original eutectic colonies (Fig. 1a). Dendritic segregation is visibly observed, but Ag precipitates are hardly found in the Cu matrix. For the specimens aged only for 1 h, Ag secondary particles are precipitated from a discontinuous precipitation reaction in the Cu matrix and tend to form some discontinuously precipitated zones adjacent to grain boundaries (Fig. 1b). The discontinuously precipitated cells extend and the precipitates slightly coarsen with increasing aging time. A

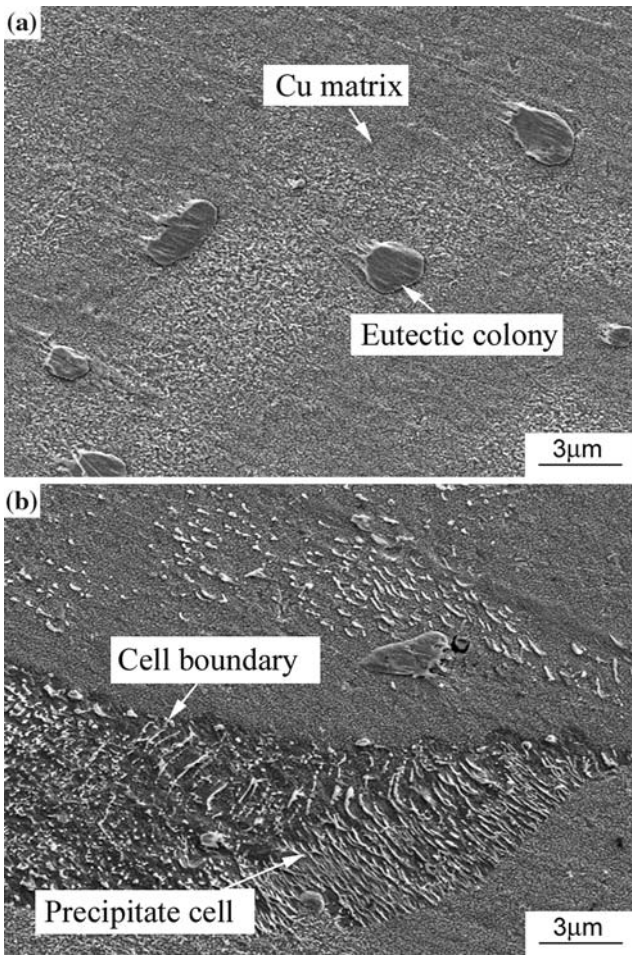


**Fig. 1** FESEM images of Cu-6 wt.% Ag (**a**) solution treated and (**b**) aged for1 h

similar discontinuous precipitation reaction was also observed in Cu-7 wt.% Ag and the discontinuous precipitates were fine due to aging at a lower temperature [20].

The morphology of Ag precipitates and selected area diffraction patterns (SADP) for the specimens aged for 16 h are shown in Fig. 2. The Ag precipitates uniformly distribute in the precipitated cells. The double-diffraction patterns are obtained from different incident directions of the electron beam. Some small spots diffracted from Ag precipitates regularly arrange around large spots diffracted from the Cu matrix. The diffraction aspect shows that there exists a perfect cube-on-cube orientation relationship, $\{111\}_{Cu}//\{111\}_{Ag}$ and $\langle 011\rangle_{Cu}//\langle 011\rangle_{Ag}$, between the Ag precipitate and the Cu matrix. This result is also well in accordance with the previous studies on Cu–Ag alloys [7, 19].

The transmission electron microscopy image of the interface between the Ag precipitate and the Cu matrix is shown in Fig. 3. Two-direction Moiré fringes can be observed in the Ag precipitate. This implies that the crystal

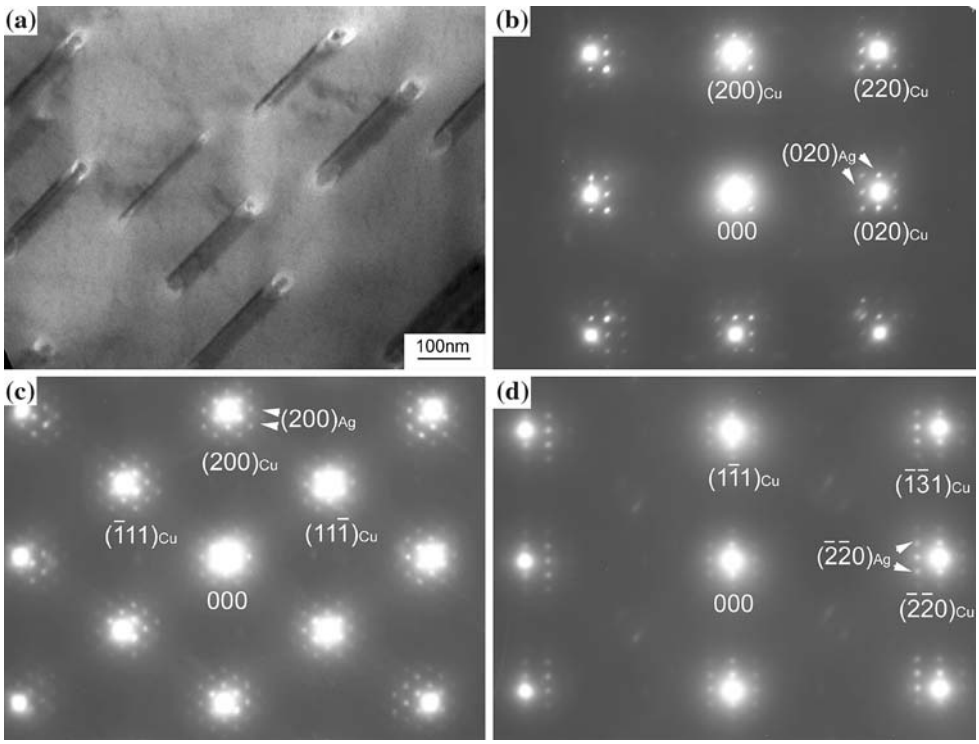


**Fig. 2** (**a**) Morphology of Ag precipitates and SADP with the electron-beam incident direction paralleled to Cu axes (**b**) [001], (**c**) [011], and (**d**) [$\bar{1}12$] in the precipitation regions of Cu-6 wt.% Ag aged for 16 h (double diffraction spots are indicated by arrows)

orientation of the Ag precipitate is the same with that of the Cu matrix. It is known that once two crystal orientations have shown parallel relationship between both face-centered cubic phases, for instance, $[111]_{Cu}//[111]_{Ag}$ and $[110]_{Cu}//[110]_{Ag}$, other crystal orientations must also be parallel relationship between both phases. Therefore, the two-direction Moiré fringes in the interface image can further confirm the presence of the cube-on-cube orientation relationship.

The images of the interface between the Ag precipitate and the Cu matrix and the corresponding inverse fast Fourier transformation (IFFT) are shown in Fig. 4. The $(100)_{Ag}$ parallels to $(100)_{Cu}$ and there are some dark regions of strain contrasts along the interface. The spacings of $(100)_{Ag}$ and $(100)_{Cu}$ are 0.204 and 0.181 nm, respectively. Some dislocations in the Cu side are regularly arranged at the interface. The average interval between the interfacial dislocations is nine plane spacings of $(100)_{Cu}$. The parallel orientation relationship and the interfacial dislocations indicate that there is a semi-coherent interface between the Ag precipitate and the Cu matrix. The lattice misfit, $\delta$, between Ag and Cu can be given by [19, 20]

$$\delta = 2(d_{Ag} - d_{Cu})/(d_{Ag} + d_{Cu}), \quad (1)$$

where $d_{Ag}$ and $d_{Cu}$ are the interplanar spacings of Ag and Cu, respectively. The lattice misfit between $(100)_{Ag}$ and $(100)_{Cu}$ is 0.119. The dislocations introduced periodically at the interface can partially release the misfit strain. However, there still are some relatively high-strain fields from the lattice distortion around the interfacial dislocations and these strain fields can form the dark regions of strain contrasts in the observation. The distance, $D_{misfit}$, between the interfacial dislocations can be calculated by [19, 20]

$$D_{misfit} = \frac{d_{Cu} + d_{Ag}}{2\delta}. \quad (2)$$

The determined average interval of the interfacial dislocations is nine plane spacings of $(100)_{Cu}$, i.e., 1.63 nm, which is in agreement with the calculated value $D_{misfit} = 1.61$ nm.

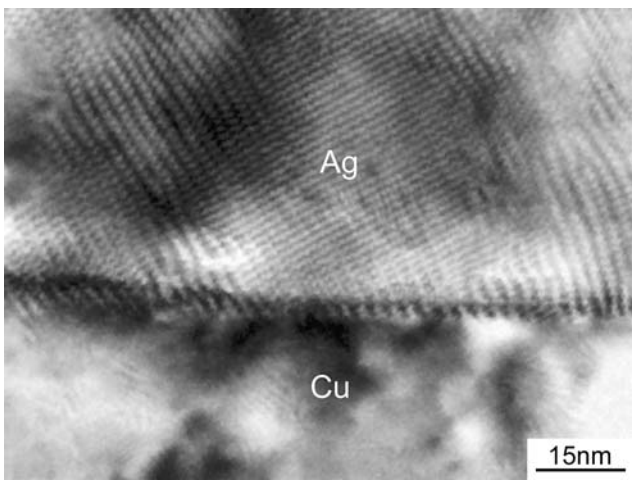


**Fig. 3** TEM image of the interface between Ag precipitate and the Cu matrix in Cu-6 wt.% Ag aged for 16 h

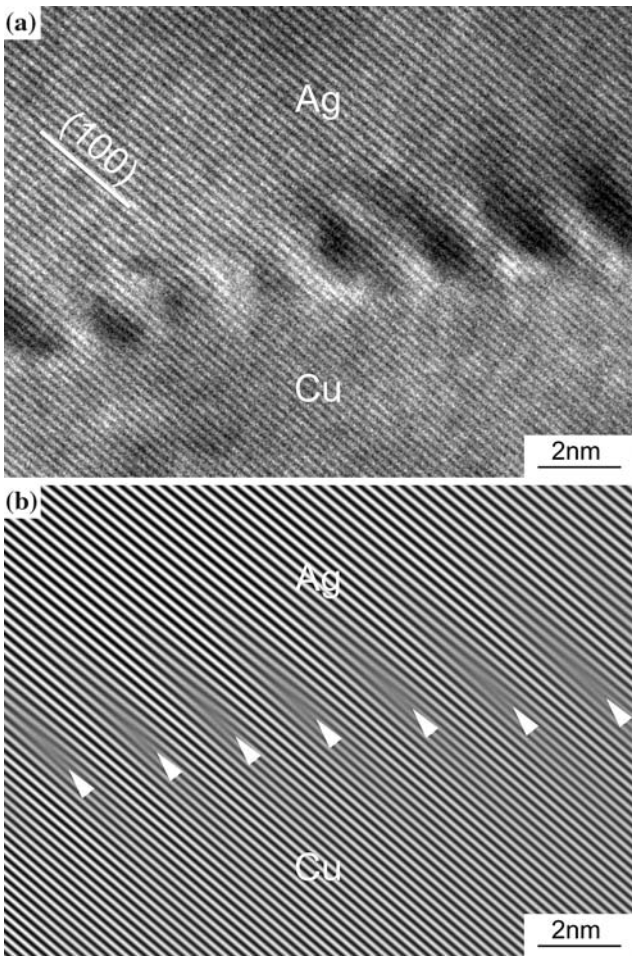


**Fig. 4** The images of (**a**) HRTEM and (**b**) corresponding IFFT of the interface with parallel (100) between Ag and Cu phases in Cu-6 wt.% Ag aged for 16 h (the arrows in the Cu side indicate interfacial dislocations)

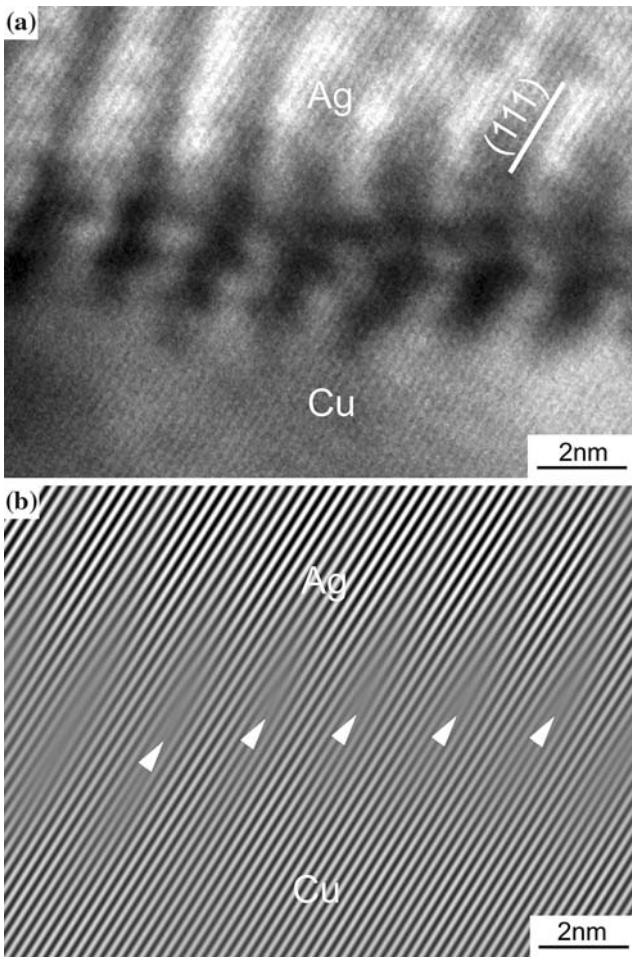


**Fig. 5** The images of (**a**) HRTEM and (**b**) corresponding IFFT of the interface with parallel (111) between Ag and Cu phases in Cu-6 wt.% Ag aged for 16 h (the arrows in the Cu side indicate interfacial dislocations)

The semi-coherent interface between the Ag precipitate and the Cu matrix can also be observed from the parallel orientation relationship between $(111)_{Ag}$ and $(111)_{Cu}$ (Fig. 5). Similarly, there are the interfacial dislocations and dark regions of the strain contrasts. The average interval between the interfacial dislocations is nine plane spacings of $(111)_{Cu}$. The spacings of $(111)_{Ag}$ and $(111)_{Cu}$ are 0.236 and 0.209 nm, respectively. The lattice misfit between $(111)_{Ag}$ and $(111)_{Cu}$ is 0.121 from Eq. 1. The distance between the interfacial dislocations is calculated to be 1.83 nm using Eq. 2. In this observation, the determined average distance between the interfacial dislocations is 1.88 nm, which is also in agreement with the calculated result.

The hardness and electrical resistivity dependent on aging time are shown in Fig. 6. The hardness increases markedly at initial aging period and slowly after 16 h. In contrast to the change of the hardness with aging time, the electrical resistivity decreases markedly at initial aging period and slowly after aging for 16 h.

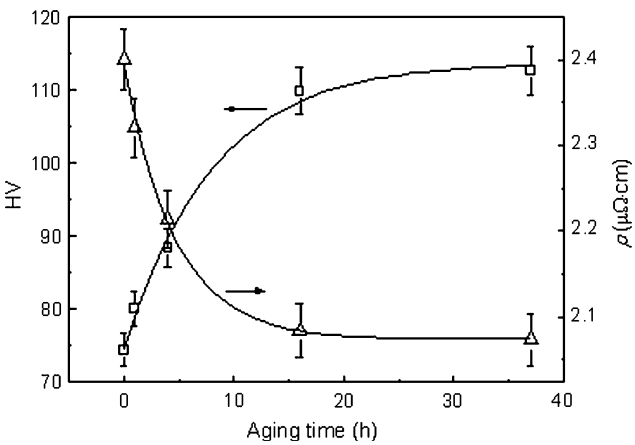


**Fig. 6** Vickers hardness and electrical resitivity of Cu-6 wt.% Ag dependent on aging time at 450 °C

## Discussion

During precipitation reaction, Ag precipitates nucleate and grow by the diffusion of Ag atoms in the Cu matrix. It has been pointed out that the habit plane of Ag precipitates in the Cu matrix is {111} since this crystallographic plane has the lowest interfacial energy [21–24]. However, it is also necessary to introduce misfit dislocations at the plane to relax the local strain since the lattice misfit between $\{111\}_{Cu}$ and $\{111\}_{Ag}$ is about 12.1%. Therefore, the semi-coherent interface between the Ag precipitate and the Cu matrix is dominantly presented in Cu-6 wt.% Ag.

Similar to the consideration in the strength prediction of composite materials, the hardness of Cu–Ag alloys can be described by the hardness summation of phase components [1, 2, 7]

$$HV_{Cu-Ag} = f_{matrix}(HV_{sol} + HV_{dis} + HV_{int}) + f_{eutectic}HV_{eutectic}, \quad (3)$$

where $f_{matrix}$ and $f_{eutectic}$ are the volume fractions for the Cu matrix and original eutectic, respectively. $HV_{sol}$, $HV_{dis}$, and $HV_{int}$ are the hardening components given from the solute, dislocation, and interface, respectively. $HV_{eutectic}$ is the hardness of the eutectic.

There are not the eutectic reaction and dislocation migration in the as-quenched structure during aging treatment. The precipitation reaction during aging can hardly affect the eutectic amount and dislocation density although aging treatment can change the volume fraction of Ag secondary particles. Therefore, the change of $HV_{Cu-Ag}$ should mainly depend on the changes of $HV_{sol}$ and $HV_{int}$ since $f_{eutectic}$ and $HV_{dis}$ are nearly constant in aging process.

$HV_{sol}$ should be a negative contribution to $HV_{Cu-Ag}$ in aging hardening because the precipitation of Ag secondary particles in aging treatment reduces the Ag concentration in the Cu matrix or impairs the solution hardening of the Cu matrix. Therefore, the improvement in the hardness level by aging treatment must only benefit from the interface hardening or a positive contribution of the $HV_{int}$ component. As a barrier of moving dislocations, the semi-coherent interface between the Ag precipitate and the Cu matrix can strongly obstruct dislocation slipping so as to harden the alloy.

The density of the semi-coherent interface increases since the area of discontinuously precipitated cells or the volume fraction of Ag precipitates increases with prolonging aging time up to 16 h. Therefore, $HV_{Cu-Ag}$ markedly increases in the aging period due to the enhanced contribution of $HV_{int}$ component to the aging hardening. After aging treatment for a long period, the precipitation reaction slows or the interface density hardly increases because the precipitation of Ag secondary particles has nearly been completed, which results in the insignificant change of the hardness with aging time after 16 h.

Precipitation reaction reduces the level of solute scattering or lattice distortion in the Cu matrix because supersaturated Ag atoms are precipitated as Ag secondary particles during aging treatment. However, the level of interface scattering should be enhanced in aging process because the presence of Ag precipitates increases the interface density. The practical results in the investigation show that the electrical resistivity decreases with the increase in aging time (Fig. 6). This implies that the reduction in solute scattering level can play a more important role in the resistivity change than the increase in interface scattering level during precipitation reaction. Similar results of the resistivity reduction from the precipitation reaction were also observed in Ni or Cu based alloys [25–27]. Moreover, the perfect cube-on-cube orientation relationship at the interface should also be responsible for the insignificant effect of interface scattering on the resistivity change in this study. The excellent matched condition of crystallographic orientation or high lattice compatibility of atomic arrangements at the interface results in low scattering capability although there are some misfit dislocations at the interface.

## Conclusions

A discontinuous precipitation occurs along the grain boundaries in the Cu matrix of Cu-6 wt.% Ag in aging treatment at 450 °C. The discontinuously precipitated cells extend with the increase in aging time.

The Ag precipitate has the cube-on-cube orientation relationship, $\{111\}_{Cu}//\{111\}_{Ag}$ and $\langle 011\rangle_{Cu}//\langle 011\rangle_{Ag}$, with the Cu matrix in the precipitation regions. There is a semi-coherent interface between Ag and Cu phases.

Dislocations are periodically introduced at the interface to release the interface misfit strain. The average distance between the interfacial dislocations is nine plane spacings of $(100)_{Cu}$ or $(111)_{Cu}$.

Aging treatment obviously improves the hardness and conductivity. The increase in the hardness and the decrease in the resistivity are more significant in the aging period before 16 h than in that after 16 h.

The increase in the interface density in the Cu matrix is mainly responsible for the hardness improvement during aging treatment. The reduction in solute concentration in the Cu matrix is mainly responsible for the conductivity improvement during aging treatment. The regular dislocation arrangement at the semi-coherent interface results in high strain resistance. The interface between the Ag precipitate and the Cu matrix shows lower scattering level than the solute atoms in the supersaturated solid solution.

**Acknowledgements** Dr Y.W. Zeng is thanked for helpful discussions about HRTEM observations. The project is financially supported from the National Natural Science Foundation of China (Grant No. 50671092).

## References

1. Hong SI, Hill MA (1998) Acta Mater 46:4111
2. Benghalem A, Morris DG (1997) Acta Mater 45:397
3. Hong SI, Hill MA (1999) Mater Sci Eng A 264:151
4. Frings PH, Bockstal LV (1995) Physica B 211:73
5. Sakai Y, Schneider-Muntau HJ (1997) Acta Mater 45:1017
6. Wood JT, Embury JD, Ashby MF (1997) Acta Mater 45:1099
7. Han K, Vasquez AA, Xin Y, Kalu PN (2003) Acta Mater 51:767
8. Han K, Embury JD, Sims JR, Campbell LJ, Schneider-Muntau HJ, Pantsyrnyi VI, Shikov A, Nikulin A, Vorobieva A (1999) Mater Sci Eng A 267:99
9. Morris DG, Benghalem A, Morris-Munoz MA (1999) Scripta Mater 41:1123
10. Zhang L, Meng L (2005) Scripta Mater 52:1187
11. Sakai Y, Inoue K, Asano T, Wada H, Maeda H (1991) Appl Phys Lett 59:2965
12. Liu JB, Meng L, Zeng YW (2006) Mater Sci Eng A 435–436:237
13. Han K, Embury JD, Petrovic JJ, Weatherly GC (1998) Acta Mater 46:4691
14. Rao G, Howe JM, Wynblatt P (1994) Scripta Metall Mater 30:731
15. Dupouy F, Snoeck E, Casanove MJ, Roucau C, Peyrade JP, Askenazy S (1996) Scripta Mater 34:1067
16. Snoeck E, Lecouturier F, Thilly L, Casanove MJ, Rakoto H, Coffe G, Askenazy S, Peyrade JP, Roucau C, Pantsyrny V, Shikov A, Nikulin A (1998) Scripta Mater 38:1643
17. Leprince-Wang Y, Han K, Huang Y, Yu-Zhan K (2003) Mater Sci Eng A 351:214
18. Lee KH, Hong SI (2004) Philos Mag Lett 84:515
19. Lee KH, Hong SI (2003) J Mater Res 18:2194
20. Hirsch P, Howe A, Nicholson RB, Pashley DW, Whelan MJ (1977) Electron microscopy of thin crystals. Krieger Publishing Company, NewYork, p 357
21. Bacher P, Wynblatt P, Foiles SM (1991) Acta Metall Mater 39:2681
22. Watanabe C, Monzen R, Nagayoshi H, Onaka S (2006) Philos Mag Lett 86:65
23. Rao G, Zhang DB, Wynblatt P (1993) Scripta Metall Mater 28:459
24. Grünberger W, Heilmaier M, Schultz L (2002) Z Metallkd 93:58
25. Lee SY, Nash P (1993) J Mater Sci 28:1957
26. Batra IS, Dey GK, Kulkarni UD, Banerjee S (2001) J Nucl Mater 299:91
27. Suzuki S, Shibutani N, Mimura K, Isshiki M, Waseda Y (2006) J Alloys Compd 417:116